Science Arts & Métiers (SAM)

is an open access repository that collects the work of Arts et Métiers Institute of Technology researchers and makes it freely available over the web where possible.

This is an author-deposited version published in: https://sam.ensam.eu
Handle ID: .http://hdl.handle.net/10985/8764

To cite this version :

Laurent BERTHE, P SAINSOT, A.A LUBRECHT, M.C BAIETTO - Plastic deformation of rough rolling contact: An experimental and numerical investigation - Wear - Vol. 312, p.51–57 - 2014

Any correspondence concerning this service should be sent to the repository Administrator : scienceouverte@ensam.eu

Arts et Métiers Institute of Technology

Plastic deformation of rough rolling contact: An experimental and numerical investigation

L. Berthe *, P. Sainsot, A.A. Lubrecht, M.C. Baietto

Université de Lyon, INSA-Lyon, CNRS, LaMCoS UMR5259, F-69621, France

A B S T R A C T

Quantifying the surface roughness evolution in contacts is a crucial step in the fatigue prediction process. Surfaces are initially conditioned by the running-in process and later altered by surface fatigue. The aim of this study is to understand and predict the evolution of the micro-geometry in the first few over-rolling cycles. Numerical predictions are validated by experiments. A major difficulty in understanding surface degradation is the measurement of the surface roughness evolution at the relevant scales. A twin disc micro-test rig, called μMag, was specially designed for this kind of analysis. The μMag allows the "in situ" observation of changes in the disc surface during interrupted tests, thus avoiding dismounting the specimens, which is a major cause of inaccuracy. The new method also maintains the relative position of the two discs. The precision of the measurements allows one to use the initial surface micro-geometry as input for the numerical contact calculation. Thus, the plastic deformation of the surfaces can be measured during the first cycles and compared to the numerical prediction. Results show a very good agreement between numerical predictions and experimental measurements.

Keywords:
Rolling contact fatigue
Running-in
Rough surfaces
Plasticity
Experimental
Numerical simulation

1. Introduction

Quantifying the surface roughness evolution in interacting contacts is a crucial step in the fatigue prediction process. Surfaces are initially conditioned by the running-in process and later altered by surface fatigue. Two difficulties are associated with running-in, the experimental analysis of the asperity and surface evolutions with time and the numerical modeling of the micro-geometry change due to wear and plastic deformation.

The authors focus on the surface evolution during the very first cycles, as important changes in the surface geometry occur rapidly. The aim of this study is to understand and predict the evolution of the micro-geometry in the first few over-rolling cycles. A major difficulty in understanding surface degradation is the measurement of the surface roughness evolution at the relevant scales. A twin disc micro-test rig, called μMag, was specially designed for this kind of analysis. The μMag allows the "in situ" observation of changes in the disc surface during test interruptions, thus avoiding dismounting the specimens, which is a major cause of location inaccuracy. The new method also maintains the relative position of the two discs. The precision of the measurements allows one to use the initial surface micro-geometry as input for the numerical contact calculation.

An extensive experimental and theoretical literature is devoted to running-in: Blau [1], Kragelski et al. [2] or the proceedings of an entire conference [3]. In the literature experimental results are mostly devoted to surface roughness and its evolution. The rough surface evolution is classically expressed using the Ra or Rq parameters and their evolution over time [4–11]. A statistical approach is also used to study rough [12,13] and fractal contacts [14,15] and to monitor functional contact parameters such as contact area and mean pressure. Evolutions of the contact models include independent spherical elasto-plastic asperity contact [16,17] or even more realistic models [18,19]. These statistical methods do not permit a deterministic surface roughness prediction.

The increase in computer performance has allowed one to use deterministic surface roughness as input data in numerical contact models to investigate the local asperity deformation. Kalker and Hills et al. [20,21] developed numerical methods to deal with non-hertzian contact problems. Following these pioneering works, numerical modeling of real rough surfaces under elastic contact conditions has been performed by Yonqing and Linqing [22], Webster and Sayles [23], Nogi and Kato [24], Polonsky and Keer [25], and Sainsot and Lubrecht [26,27] using a variety of techniques including FFT and multigrid. Extensions have been developed

* Corresponding author.
E-mail address: laure.berthe@insa-lyon.fr (L. Berthe).

introducing plasticity in semi-analytical methods [28–31]. The direct determination of the stabilized mechanical state induced by repeated rolling contact in the case of shakedown (elastic or plastic) was proposed [32] and relies on the steady state assumption in the moving contact reference frame. This direct stationary method calculate the steady state solution at once. For the three dimensional rolling contact problem, a numerical procedure based on finite elements and Fourier expansion was developed to reduce the computational cost [33]. More recently, improvement of computer facilities has allowed the use of Finite Element Methods [34–37], employing a large panel of constitutive laws, but computing times remain significant [38].

Concerning rolling contacts, a combined experimental and numerical approach using surface roughness was presented by Hooke and Li [39]. Surface roughness measurements were used as input data for 2D numerical simulations to determine the corresponding EHL pressure distributions and stresses. However, very rough surfaces and relatively soft materials were used to avoid important relative measurement errors.

The purpose of this paper is to predict the surface topography at the roughness scale, after the running-in process of contacting metal surfaces under pure rolling conditions. Experiments are performed, using a 52100 steel discs with a Ra roughness of 0.6 and 0.01 μm. The material and surface geometry are selected as they are close to industrial applications. The surface roughness evolution is monitored during the beginning of the running-in process. The measurement technique developed is described in Section 1. Section 2 briefly presents the elastoplastic contact model developed by Mayeur et al. [40]. This model is based on the direct stationary method proposed by Zarka et al. [41] and Inglebert et al. [42,43] to determine the stabilized state of the material under cyclic loading. It is used to determine the contact pressure distribution, the asperity plastic deformation and the subsurface stresses. To validate the model, the experimental plastically deformed geometry is compared to the numerical elastoplastic prediction.

2. Experimental

2.1. Test rig description

A two-disc machine named μMaG has been developed in the lab to perform detailed studies of rough surfaces in contact. This test rig allows one to: (i) perform tests one cycle at the time, (ii) to maintain the relative position of the disks during surface measurement, (iii) to measure exactly the same surface zone each time and (iv) to reposition numerically the smooth and rough surfaces with respect to one other, with a micrometer precision.

(i) The test machine (Fig. 1) has a stepper motor and a position sensor of 65,536 points per revolution.
(ii) The disk unit (comprised of upper and lower disc) can be removed from the test rig whilst maintaining the relative position of the two discs. The disc unit height is only 5 cm and it can be positioned under an optical microscope or roughness analyser (Fig. 2). As such the roughness evolution can be observed cycle after cycle.
(iii) Relocation to one micrometer, allows optical microscope measurements or roughness analysis to study exactly the same surface area (Fig. 3a). Fig. 3b shows the micro-geometry after 1 and 20 cycles of the smooth disk. The roughness outside the track ($y < -200$ μm or $y > 200$ μm) does not evolve and superposes (Fig. 3c).
(iv) Finally, contact calculations between the rough and smooth surfaces are carried out (Fig. 4).

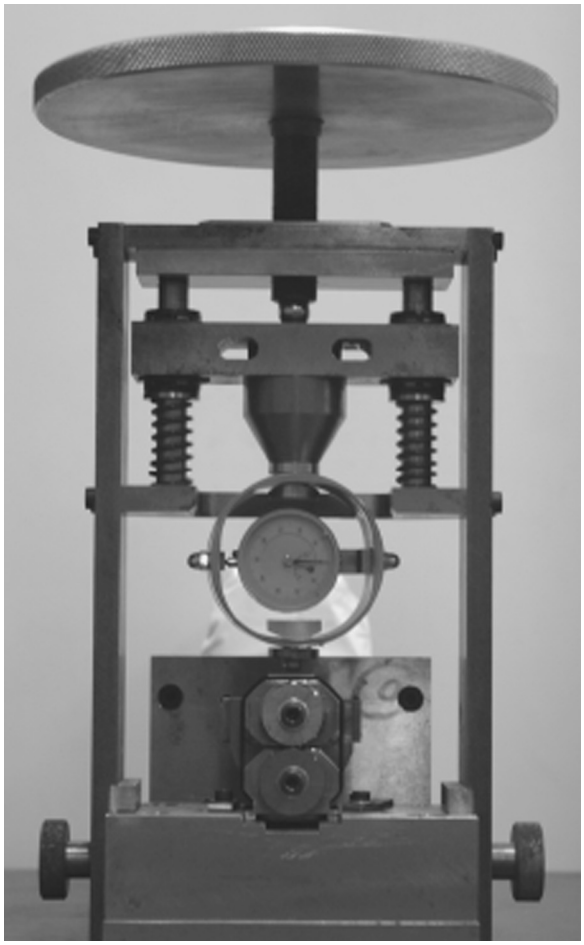

Fig. 1. The μMaG.

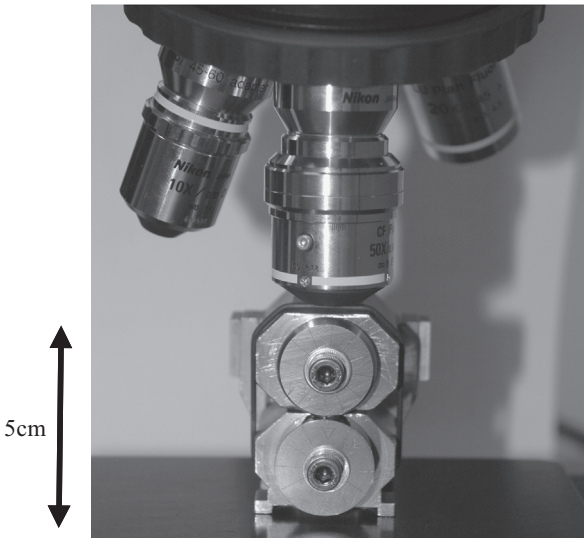

Fig. 2. Roughness analyser/Optical microscope.

The stepper motor directly drives the smooth, lower disk. The rough upper disk is entrained by friction and pure rolling conditions are considered for the rest of the work.

2.2. Operating conditions

The two discs are made of 52100 steel (Table 1). The upper disc is crowned and longitudinal grooves were machined with a 0.6 μm

Ra roughness. The lower disc is cylindrical and polished to a roughness of 0.01 μm Ra.

The contact is dry, no lubricant is used and the rotational velocity is very low: one revolution per minute. The two discs are very close to pure rolling, virtually excluding any third body generation. The surface transformation is limited to the generation of residual stresses, due to plastic deformation, in a very shallow subsurface layer. The applied normal load is 121 N, yielding a maximum Hertzian pressure of 2 GPa and a contact radius of 170 μm (Table 2).

The maximum Hertz pressure p_0 for yield is given by $(p_0)_Y=3.2k$ and $(p_0)_Y=2.8k$ (Tresca, Von Mises), where k is the yield stress in simple shear equal to 1 GPa [6]. This pressure value implies a globally elastic contact. Obviously, at the scale of the roughness, the contact will be locally plastic

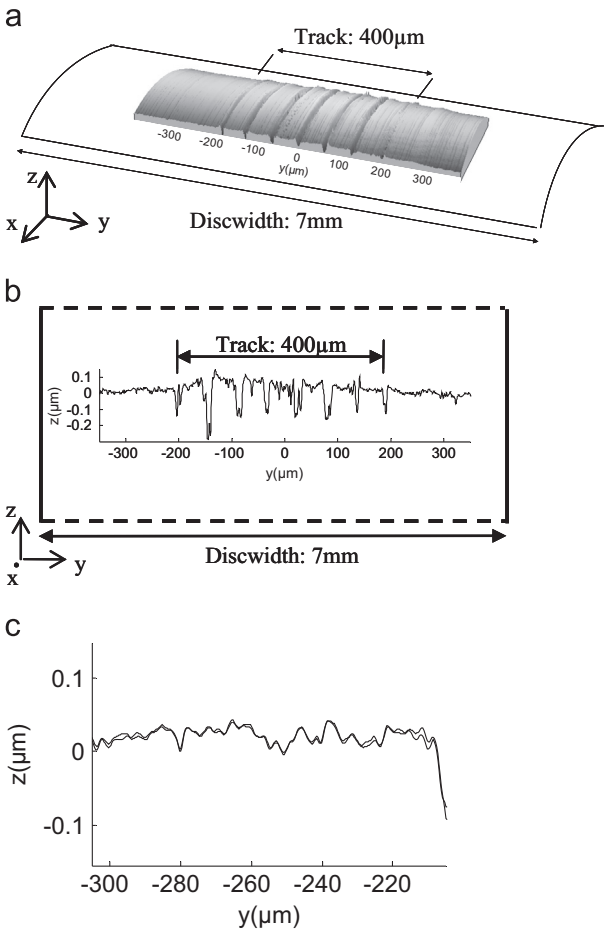

Fig. 3. Optical microscope measurements and relocation of disc profiles. (a) Sketch of the contact track of smooth disc topography, (b) sketch of the contact track of smooth disc profile, and (c) superposition of smooth disc profiles outside the track after 1 and 20 cycles.

2.3. Experimental results

This work analyses the surface roughness evolution versus the number of cycles. During each cycle the asperity tops of the rough disc indent the smooth disc surface over a domain ranging from $y=-200$ μm to $y=200$ μm.

The tests are interrupted after a certain number of cycles. At each interruption, pictures are taken and two dimension surface topography measurements are performed (Fig. 3a). One dimensional roughness profiles are extracted (Fig. 3b) from the surface topography at the same location (± 0.5 μm) after 0, 1, 10 and 20 cycles (Fig. 5) of both rough and smooth discs. The precision of the relocation is demonstrated by the superposition of the roughness profiles outside the track.

During the test, the height of the asperities is reduced as shown in Fig. 5(c) and a zoom (d). The reduction is not the same for all the asperities, as it depends on initial height and position within the contact. This height reduction concurs with the formation of grooves on the smooth disc; the groove depth is roughly equal to the peak height decrease. Careful surface observation showed no signs of wear.

More precisely, the geometrical evolution of the rough and smooth disc can be described by:

- An increase of the contact area and an increase in the number of asperities in contact, from 5 at cycle 1 to 8 at cycle 10. The real area of contact increases roughly by 8%.
- A decrease of the height of the asperities, due to plastic deformation.
- On the smooth disc, grooves are formed.
- These grooves are surrounded by shoulders. Their height depends on the depth and shape of the groove shown in Fig. 5(a) and a zoom (b). This demonstrates that material flow occurs during contact.

Table 1
Material properties.

Material	52100 Steel
E: Young's Modulus	210 GPa
ν: Poisson's ratio	0.3
k: Elastic shear limit	1 GPa
C: Hardening modulus	27 GPa

Table 2
Disc characteristics.

Disc	Rx (mm)	Ry (mm)	Width (mm)	Ra (μm)	Surface finish
Crowned:	12.5	6.25	7	0.6	Striated
Cylindrical:	12.5	∞	7	0.01	Polished

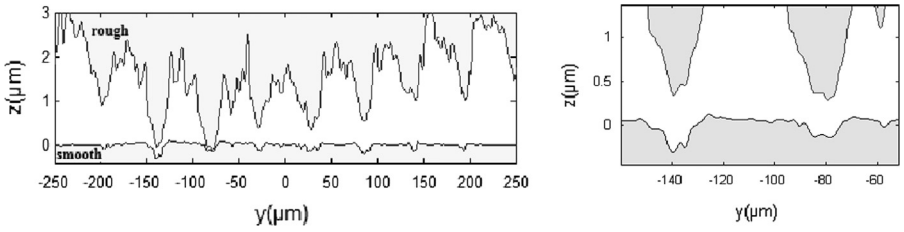

Fig. 4. Relative position of smooth and rough disk profiles after 10 cycles.

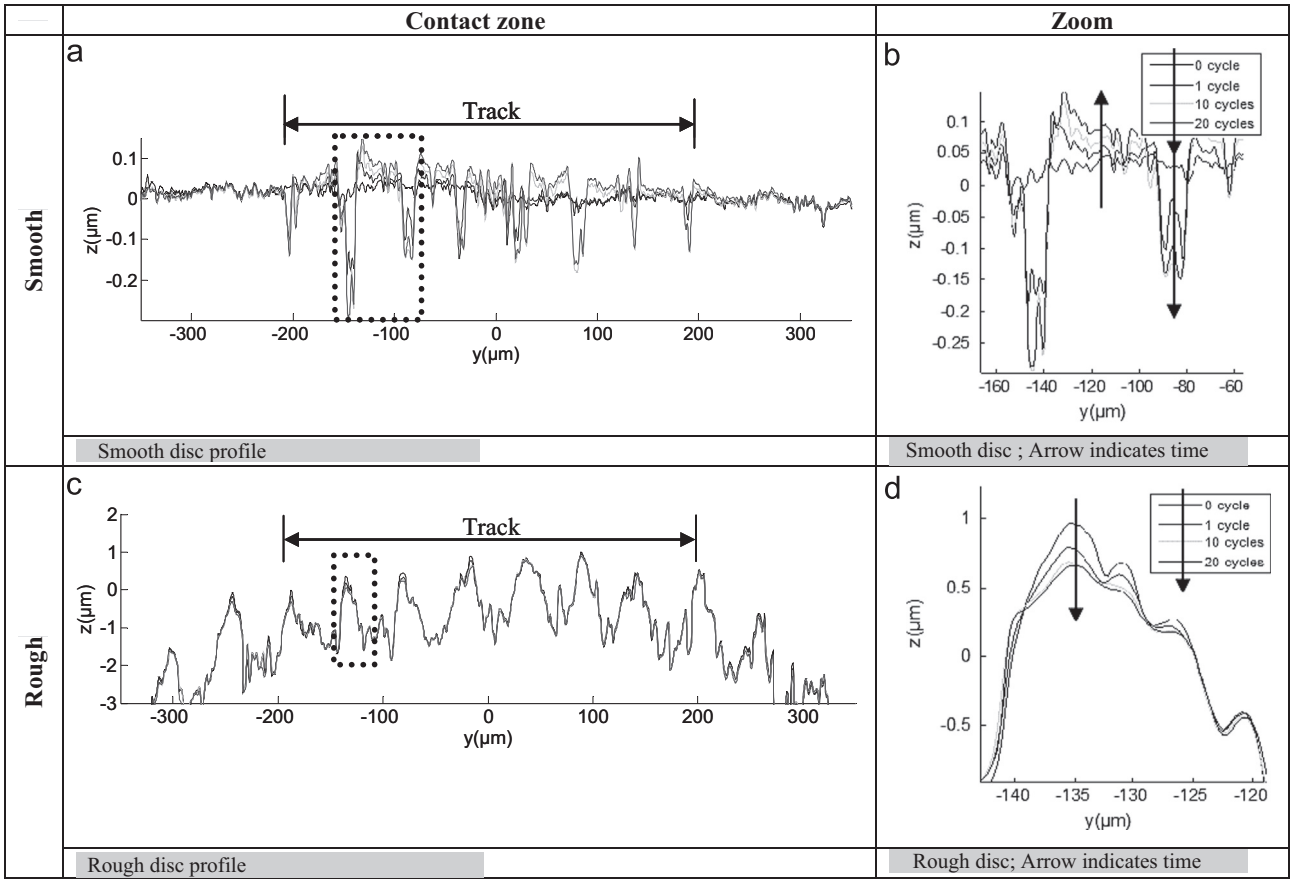

Fig. 5. Surface profile evolution versus cycles (0, 1, 10 and 20 cycles).

A literature survey was carried out, to decide on the number of cycles, necessary to reach an elastic shakedown state. Once the elastic limit is exceeded, plastic deformation takes place and generates residual stresses. These are essentially protective, as the material strain-hardens and thus increases its effective yield stress [6,44]. After a few cycles, the residual stresses have reached such values that subsequent load passes result in entirely elastic deformation. Hence, a purely elastic cyclic steady state is reached.

For a circular elasto-plastic contact and an isotropic material, Johnson [6] stated that the residual stresses build up very quickly and a steady state is virtually reached after four or five load cycles.

Jiang et al. [38] performed a 3d finite element study of a spherical rolling contact and considered a material obeying a kinematic hardening constitutive law. For a mild steel (1070 steel, 192HB), it was shown that the residual stresses stabilise after a finite number of load cycles. They also performed simplified 2d finite element analysis to obtain results in a shorter time. After approximately 30 cycles, they obtained a stabilised state. The residual stress values after the tenth and twentieth cycle were found to be 8 and 3% less than the stabilised value.

Under repeated spherical indentation and for a material with a linear isotropic hardening constitutive law, Kadin et al. [45] showed that a steady state is reached after the first loading–unloading cycle and that the subsequent loading cycles become fully elastic.

In 2010, Li et al. [46] studied the effect of asperity flattening during cyclic normal loading of rough spherical contacts. Li et al. also showed, that after the first cycle, a tendency towards reduced plastic deformation with subsequent load cycles occurs (elastic shakedown).

Concluding, the different models and different constitutive laws used in previous work show that elastic shakedown is reached after a dozen load cycles. The material used in this paper is a 51200 steel and obeys a kinematic hardening constitutive law whose characteristics are given in Table 1. The experiments were performed under pure rolling conditions and one observes that the roughness profiles were very close after 10 and 20 cycles. We assume the 10th cycle to be our stabilised reference state, for our numerical calculations.

2.4. Partial conclusion

A new twin-disc was built to analyse the roughness topography evolution with load cycles. Because of its small dimensions, the surface topography measurements can be performed, without separating the contacting discs. This opens the possibility to study the surface evolution cycle after cycle.

It was observed that after 10 cycles the roughness topography evolved little, and that local plastic deformations ceased to occur. The next section will use an elasto-plastic contact model to simulate the contact between the measured rough surfaces. Measurements of the contacting surfaces are taken after 0 and 10 cycles. The measured smooth and rough profiles after 0 cycles are used as input in the numerical simulation. The next section is devoted to the numerical simulation of the experiments. A 3d numerical elastoplastic model for rough contacts is briefly presented. The pressure field and the subsurface stresses are computed. The deformed surface is compared to the measured surface after 10 cycles. The stabilized state is reached after one single calculation: hence no intermediate measured profiles are used.

3. Numerical model

3.1. Elasto-plastic model for rough rolling contact

In the case of repeated contact loadings, the occurrence of damage implies plastic strain. Finite element methods and semi-analytical methods are generally used to perform elastic–plastic analysis of rough contacting rolling bodies. The former is able to deal with complex geometrical designs with actual roughness and advanced constitutive laws can be used. Nevertheless, the mesh refinement required to perform analysis at the roughness scale leads to very lengthy calculations. The computing time is further augmented by the incremental step by step integration employed to calculate the stabilised state. Semi-analytical methods are efficient and robust, but limited to simple geometries (like half planes, spheres, cylinders) and classical elasto-plastic constitutive laws [28–31]. Specific computational techniques allow one to reduce the calculation times, particularly by replacing classical incremental methods by stationary methods [32].

The stationary method, based on the work of Zarka et al. [41], Inglebert et al. [42,43] and Dang Van et al. [32], allows the determination of the asymptotic response of the structure without following the loading step by step. It applies to a structure subjected to contact loads moving with a velocity V in a fixed direction. Assuming a steady state in a reference frame moving with the load, the equations governing the problem are written in the moving frame related to the load. This allows one to replace time derivatives by space derivatives along the direction of motion. In this method, both the load and the structure are stationary. The stabilised state caused by the cyclic load is reached directly. This original scheme of integration has been employed in finite element methods [32,41–43].

This stationary method has been implemented in a semi-analytical elasto-plastic model developed by Mayeur et al. [40]. This computational model is able to deal efficiently with 3D rough rolling contact. The material behaviour adopted is a Von-Mises elastic–plastic model with linear kinematic and isotropic hardening. These assumptions are quite suitable to represent a metal, especially for cyclic loading, and are easy to implement in a numerical procedure.

The yield condition is defined by

$$f(\sigma_{ij},\ \in^{p}_{ij}) = \sqrt{\frac{3}{2}(s_{ij} - C \in^{p}_{ij})(s_{ij} - C \in^{p}_{ij})} \le \sigma_y,\ \text{with } s_{ij} = \sigma_{ij} - \frac{1}{3}\sigma_{kk}\delta_{ij} \tag{1}$$

where s_{ij} are the deviatoric stress tensor components, ϵ^{p}_{ij} the plastic strain tensor components, C the hardening modulus, σ_y the elastic limit in traction and δ_{ij} the Kronecker symbol. In a nine dimensional space (the deviatoric stress space), the elastic domain is represented by a sphere of radius $\sqrt{2/3}\sigma_y$ which has a translation proportional to plastic strain rates.

Plastic flow is governed by

$$\dot{\in}^{p}_{ij} = \frac{3}{2C\sigma_y^2}[(s_{ij} - C \in^{p}_{ij})\dot{s}_{ij}](s_{ij} - C \in^{p}_{ij}),\ \textit{if}\quad f(\sigma_{ij},\ \in^{p}_{ij}) = \sigma_y \textit{ and } \frac{\partial f}{\partial s_{ij}}\dot{s}_{ij} > 0 \tag{2}$$

where the dot denotes the time derivative of the variables.

The elasto-plastic problem is solved with the simplified method proposed by Zarka et al. [41], Inglebert et al. [42,43] and Dang Van et al. [32].

This method has been applied to the 3D rough rolling contact, with roughness ridges in the rolling direction x (hence, constant roughness in the x direction). Under these conditions, the residual stresses and deformations are constant in the x direction.

Nevertheless, the solution of the contact problem and the residual stresses are calculated in 3D. The numerical procedure is outlined in Fig. 6.

In the current paper, this semi-analytical model has been used. The two initial surface profiles are extracted from the rough and smooth discs and the experimental test conditions are numerically reproduced. The numerical method is based on a boundary integral formulation for an elastic half plane. Only the zone where plasticity may occur is discretised and the remaining domain is considered elastic. This allows a significant gain in computing time compared to the Dang Van et al. study [32].

3.2. Simulation of experimental tests

The "Mayeur method" allows one to treat a three dimensional rough rolling contact when the roughness consists of ridges oriented along the rolling direction. This configuration is representative for the smooth and rough disc contact, because of the manufacturing process.

The size of the plastic domain is $400 \times 400 \times 50\ \mu m^3$ and is identical for both the smooth and rough disc. The mesh size is $4 \times 0.5 \times 0.5\ \mu m^3$, assuming longitudinal roughness in the x direction.

The elastic shear limit used for the plastic behaviour is $k = 1$ GPa and the hardening modulus is $C = 27$ GPa (Table 1). The geometry and the load are those found in the experiment, see Section 1. The computing time on a standard laptop computer is approximately 2 h.

3.3. Solution of the real rough contact

To understand the impact of the plastic deformation on the contact behaviour, one analyses the pressure and stress distribution.

The upper part of Fig. 7 shows the contact pressures using the initial roughness geometry and applying 10 numerical load cycles. The maximum pressure is half the value obtained with a pure elastic calculation and the initial roughness geometry. Local high pressures arise at contacting asperity tops. These local pressures exceed 6 GPa with a maximum of 10 GPa.

The lower part shows the Von Mises stress distribution. The points where $\sigma_{VM}/k > 1$ in grey correspond to the plastically deformed volume and 98% of these points have a value inferior to 2. The points where $\sigma_{VM}/k > 2$ coincide with a pressure exceeding 8.1 GPa. The pressure integral over these points represents only 0.2% of the total load.

This result confirms the elastic shakedown hypothesis that assumes $\sigma_{VM}/k < 2$.

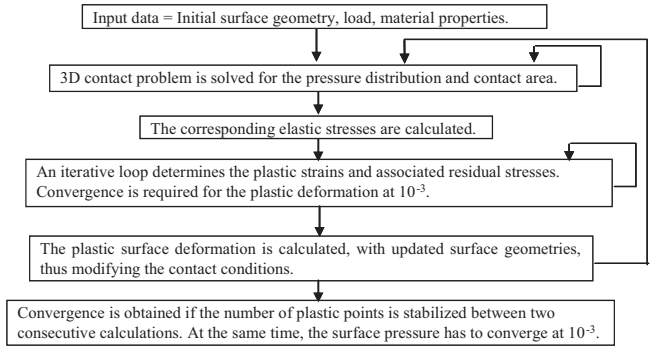

Fig. 6. Flowchart of the elasto-plastic model by Mayeur et al. [40].

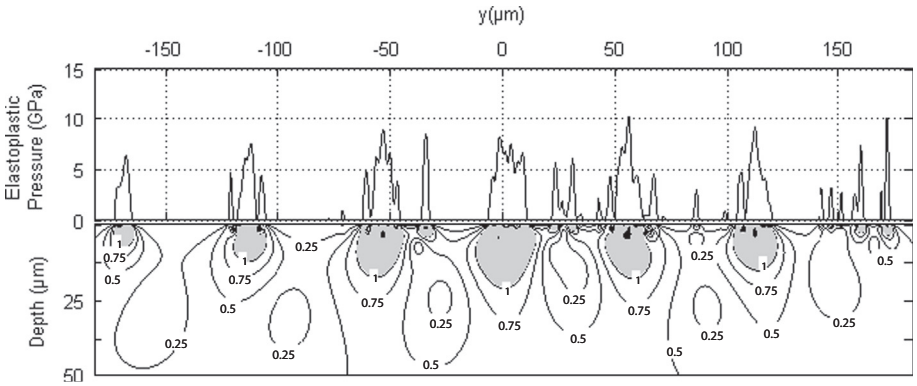

Fig. 7. Elastoplastic pressure distribution and σ_{VM}/k isovalues at $x=0$.

Plastic Zone: $1<\sigma_{VM}/k<2$

$\sigma_{VM}/k>2$

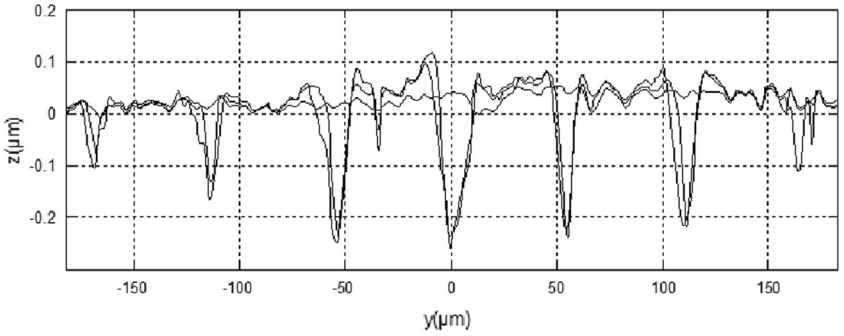

Fig. 8. Evolution of a smooth disc: initial profile, profile measured after 10 cycles, profile computed after 10 cycles. The main point is that the difference between the measured and the computed profiles is very small. The initial profile has no grooves.

3.4. Comparison of the experimental and numerical results

Fig. 8 presents 3 profiles: the initial profile, the profile measured after 10 cycles and the profile predicted by the numerical model after 10 cycles. The difference between the measured and the predicted profiles should be analysed in the light of the deformation from the smooth surface.

From a global point of view, a good correlation is obtained between the measured profile surface and the simulated one. Indeed, the crushing of material is similar. Material shoulders appear on both sides of the grooves.

More precisely, the grooves appear at the correct position, thereby confirming the precision of the relocation procedure. The mean depth of the five deepest grooves is 0.2 μm, 20 times larger than the initial surface roughness. Between each groove, the initial surface roughness is preserved, in spite of the shoulder formation.

The good agreement between experiments and the numerical prediction allows one to validate the numerical model.

4. Conclusion

The initial running-in process was studied experimentally and numerically. A dedicated twin-disc test rig, called μMaG, has been developed to analyse the surface evolution over the very first loading cycles, as important changes in the surface topography occur rapidly. The μMaG allows the in-situ observation of changes in the disc during test interruptions, thus avoiding the dismounting of the specimens, which is a major cause of inaccuracy. This method allows one to maintain the relative position of the two discs. A rough and a smooth disc were used. The Ra roughness was 0.6 μm for the rough disc and 0.01 μm for the smooth disc. The rough disc is crowned with longitudinal grooves and the smooth disc is a polished cylindrical disc. Measurements of each surface were carried out during the first twenty cycles. The measurements show a quasi stabilized surface geometry between 10 and 20 cycles.

The measured initial surfaces are used as input for numerical simulations. An elasto-plastic model based on the direct stabilized method was used to determine the evolution between the initial surface and the surface measured after 10 cycles. It was shown that the elasto-plastic model predicts the contact area and the surface topography evolution of the smooth surface very well. Moreover the numerical model predicts the plastic residual stresses and strains in the subsurface.

The elasto-plastic model is robust and computationally efficient and in spite of its simplicity it provides a detailed roughness prediction especially of the material shoulders.

The next step is to extend the analysis of the running-in process and to study the rough surface degradation up to one million cycles.

References

[1] P.J. Blau, Friction and Wear Transitions of Materials: Break-in, Run-in, Wear-in, Noyes Publications, 1989.
[2] I. Kragelsky, N. Dobychina, V. Kombalov, Friction and Wear: Calculation Methods, Elsevier Science & Technology, 1982.
[3] D. Dowson. University of Leeds. Institute of Tribology, Institut National des Sciences Appliquées de Lyon, The Running-in Process in Tribology, in: Proceedings of the 8th Leeds–Lyon Symposium on Tribology held in the

Institut National Des Sciences Appliquées de Lyon, France, 8–11 September, 1981, Buttersworth, 1982.
[4] E.J. Abbott, F.A. Firestone, Specifying surface quality, Mech. Eng. 55 (1933) 569.
[5] K.L. Woo, T.R. Thomas, Contact of rough surfaces: a review of experimental work, Wear 58 (2) (1980) 331–340.
[6] K.L. Johnson, Contact Mechanics, Cambridge University Press, 1987.
[7] W. Wang, P.L. Wong, J.B. Luo, Z. Zhang, A new optical measurement on moving surface, Tribol. Int. 31 (5) (1998) 281–287.
[8] W. Wang, P.L. Wong, Z. Zhang, Experimental study of the real time change in surface roughness during running-in for PEHL contacts, Wear 244 (1–2) (2000) 140–146.
[9] B. Bhushan, Surface roughness analysis and measurement techniques, Modern Tribology Handbook 1 (2001) 49–119.
[10] J.-H. Horng, M.-L. Len, J.-S. Lee, The contact characteristics of rough surfaces in line contact during running-in process, Wear 253 (2002) 899–913.
[11] J. Jounini, P. Revel, P.-E. Mazeran, M. Bigerelle, The ability of precision hard turning to increase rolling contact fatigue life, Tribol. Int. 59 (2013) 141–146.
[12] J.A. Greenwood J.B.P. Williamson, Contact of nominally flat surfaces, in: Proceedings of the Royal Society, London, 109 (4), 1966, 618–626.
[13] J.A. Greenwood, J.J. Wu, Surface roughness and contact: an apology, Meccanica 36 (6) (2001) 617–630.
[14] B. Persson, O. Albohr, U. Tartaglino, A. Volokitin, E. Tosatti, On the nature of surface roughness with application to contact mechanics, sealing, rubber friction and adhesion, J. Phys.: Condens. Matter 17 (1) (2005) R1–R62.
[15] C. Vallet, D. Lasseux, H. Zahouani, P. Sainsot, Sampling effect on contact and transport properties between fractal surfaces, Tribol. Int. 42 (8) (2009) 1132–1145.
[16] L. Li, I. Etsion, F.E. Talke, Elastic–plastic spherical contact modeling including roughness effects, Tribol. Lett. 40 (3) (2010) 357–363.
[17] R.L. Jackson, I. Green, A statistical model of elasto-plastic asperity contact between rough surfaces, Tribol. Int. 39 (9) (2006) 906–914.
[18] M. Ciavarella, J.A. Greenwood, M. Paggi, Inclusion of interaction in the Greenwood and Williamson contact theory, Wear 265 (5) (2008) 729–734.
[19] K. Komvopoulos, D.H. Choi, Elastic finite element analysis of muli-asperity contacts, ASME J. Tribol. 114 (1992) 823–831.
[20] J.J. Kalker, Three-Dimensional Elastic Bodies in Rolling Contact, Kluwer Academic Pubhshers, Dordrecht (1990) 314.
[21] D.A. Hills, D. Nowell, A. Sackfield, Chapter 14—rough contacts and numerical methods, in: D. Hills, D. Nowell, A. Sackfield (Eds.), Mechanics of Elastic Contacts, Butterworth-Heinemann, 1993, pp. 392–438.
[22] J. Yonqing, Z. Linqing, A full numerical solution for the elastic contact of three dimensional real rough surfaces, Wear 157 (1992) 151–161.
[23] M.N. Webster, R.S. Sayles, A numerical model for the elastic frictonless contact of real rough surfaces, ASME J. Tribol. 108 (1986) 314–320.
[24] T. Nogi, T. Kato, Influence of a hard surface layer on the limit of elastic contact—Part I: analysis using a real surface model, ASME J. Tribol. 119 (1997) 493–500.
[25] I.A. Polonsky, L.M. Keer, A fast and accurate method for numerical analysis of elastic layered contacts, ASME J. Tribol. 122 (2000) 30–35.
[26] P. Sainsot, A.A. Lubrecht, Efficient solution of the dry contact of rough surfaces: a comparison of FFT and MG methods, Proc. IMechE Part J, J. Eng. Tribol. 225 (6) (2011) 441–448.
[27] P. Sainsot, Analytical stresses in rough contacts, Proc. IMechE Part C, J. Mech. Eng. Sci. 225 (2) (2011) 274–279.
[28] C. Jacq, D. Nelias, G. Lormand, D. Girodin, Development of three-dimensional semi-analytical elastic–plastic contact code, ASME J. Tribol. 124 (2002) 653–667.
[29] P. Sainsot, C. Jacq, D. Nélias, A numerical model for elastoplastic rough contact, Computer Modeling in Engineering and Sciences, 4, Tech Science Press (2002) 497–506.
[30] F. Wang, L.M. Keer, Numerical simulation for three dimensional elastic-plastic contact with hardening behavior, ASME J. Tribol. 127 (2005) 494–502.
[31] T. Chaise, D. Nelias, Contact pressure and residual strain in 3d elasto-plastic rolling contact for a circular or elliptical point contact, J. Tribol. 133 (4) (2011).
[32] K. Dang Van, M.H. Maitournam, Steady-state flow in classical elastoplasticity: applications to repeated rolling and sliding contact, J. Mech. Phys. Solids 41 (11) (1993) 1691–1710.
[33] K. Dang Van, M.H. Maitournam, On some recent trends in modelling of contact fatigue and wear in rail, Wear 253 (2002) 219–227.
[34] V.A. Yastrebov, J. Durand, H. Proudhon, G. Cailletaud, Rough surface contact analysis by means of the finite element method and of a new reduced model, C. R. Méc. 339 (7–8) (2011) 473–490.
[35] L. Pei, S. Hyun, J.F. Molinari, M.O. Robbins, November finite element modeling of elasto-plastic contact between rough surfaces, J. Mech. Phys. Solids 53 (11) (2005) 2385–2409.
[36] K. Poulios, P. Klit, Implementation and applications of a finite-element model for the contact between rough surfaces, Wear 303 (1) (2013) 1–8.
[37] M.J. Bryant, H.P. Evans, R.W. Snidle, Plastic deformation in rough surface line contact—a finite element study, Tribol. Int. 46 (1) (2012) 269–278.
[38] Y. Jiang, B. Xu, H. Sehitoglu, Three-dimensional elastic-plastic stress analysis of rolling contact, ASME J. Tribol. 124 (4) (2002) 699–708.
[39] C.J. Hooke, K.Y. Li, An experimental study of the relationship between surface roughness and stress in EHL contacts, Tribol. Interface Eng. Ser. 38 (2000) 735–746.
[40] C. Mayeur, P. Sainsot, L. Flamand, A numerical elastoplastic model for rough contact, ASME J. Tribol. 117 (3) (1995) 422–429.
[41] J. Zarka, J.J. Engel, G. Inglebert, On a simplified inelastic analysis of structures, Nucl. Eng. Des. 57 (1980) 333–368.
[42] G. Inglebert, J. Frelat, J.M. Proix, Structures under cyclic loading, Arch. Mech. 37 (4–5) (1985) 365–382.
[43] G. Inglebert, J. Frelat, Quick analysis of inelastic structures using a simplified method, Nucl. Eng. Des. 116 (3) (1989) 281–291.
[44] A. Kapoor, K.L. Johnson, Effect of changes in contact geometry on shakedown of surfaces in rolling/sliding contact, Int. Mech. Sci. 34 (3) (1992) 223–239.
[45] Y. Kadin, Y. Kligerman, I. Etsion, Multiple loading–unloading of an elastic–plastic spherical contact, Int. J. Solids Struct. 43 (22) (2006) 7119–7127.
[46] L. Li, A. Ovcharenko, I. Etsion, F. Talke, The effect of asperity flattening during cyclic normal loading of a rough spherical contact, Tribol. Lett. 40 (3) (2010) 347–355.